

Received	2025/05/20	تم استلام الورقة العلمية في
Accepted	2025/06/11	تم قبول الورقة العلمية في
Published	2025/06/12	تم نشر الورقة العلمية في

## Effects of Sampling on Controlled Signals Using Matlab

Nasser B. Ekreem<sup>1\*</sup>, Samieh A. Abu Saad<sup>2</sup>, Samaher A. Elnajar<sup>3</sup>,  
Mostafa B. Abuitbel<sup>4</sup>

<sup>1</sup> Department of Electrical and Electronic Engineering, Faculty of Engineering, Azzaytuna University-Tarhuna - Libya

<sup>2</sup> Department of Control Engineering, College of Electronic Technology-Tripoli - Libya

<sup>3</sup> Department of Control Engineering, College of Electronic Technology-Tripoli - Libya

<sup>4</sup> Department of Electrical and Electronic Engineering, Faculty of Engineering, Azzaytuna University-Tarhuna - Libya

\*Corresponding author email: [nekreem@gmail.com](mailto:nekreem@gmail.com)

### Abstract

Sampling is the process of converting continuous time signals into discrete numerical values, is fundamental in digital control systems. Accurate sampling is critical to ensure that the discrete signals used in digital controllers strictly represent the original continuous signals without distortion. This paper presents a comparative analysis of analog signals sampled at rates above and below the Nyquist rate, emphasizing the impact on signal integrity in both time and frequency domains. Using MATLAB simulations, the spectrum of sampled signals is examined to demonstrate how undersampling leads to aliasing, a phenomenon that introduces distortion and degrades control system performance and may lead to instability. The study highlights the importance of selecting appropriate sampling rates in digital control to avoid aliasing effects, ensuring an accurate signal representation for reliable control actions. Simulation results, including MATLAB-generated plots, illustrate the relationship between sampling rate, aliasing, and signal fidelity, providing valuable insights for practitioners designing digital control systems.

**Keywords:** Sampling, Digital Control, Aliasing, Nyquist Rate, Signal Spectrum, Fourier Transform, Discrete Signals.

## تأثيرات أخذ العينات على إشارات التحكم باستخدام ماتلاب

نصر بشير عكريم<sup>1\*</sup>، سميح العماري أبوسعد<sup>2</sup>، سماهر علي النجار<sup>3</sup>،  
مصطفى بن عروس أبوطييل<sup>4</sup>

<sup>1</sup>قسم الهندسة الكهربائية والإلكترونية، كلية الهندسة، جامعة الزيتونة، تروونه - ليبيا

<sup>2</sup>قسم هندسة التحكم الآلي، كلية التقنية الإلكترونية، طرابلس - ليبيا

<sup>3</sup>قسم هندسة التحكم الآلي، كلية التقنية الإلكترونية، طرابلس - ليبيا

<sup>4</sup>قسم الهندسة الكهربائية والإلكترونية، كلية الهندسة، جامعة الزيتونة، تروونه - ليبيا

### الملخص

أخذ العينات، عملية تحويل الإشارات الزمنية المتصلة إلى قيم رقمية متقطعة، تعد هذه العملية أساسية في نظم التحكم الرقمية، فهذه العملية تلعب دورا هاما للتأكد من أن الإشارات المنقطعة الداخلة إلى المتحكمات الرقمية تمثل بشكل دقيق الإشارات الأصلية دون تشويه وتحتوي جميع البيانات اللازمة المنقولة من الإشارات الأصلية. تقدم هذه الورقة تحليلاً مقارناً بين الإشارات التماثلية (المستمرة) والإشارات التي تم انتاجها من خلال محاكات عملية أخذ العينات بترددات عند أعلى وأقل من تردد نيكويست، مع التأكيد على مدى تأثير هذه العملية على سلامة الإشارة في المستويين الزمني والترددي. يتم باستخدام بيئة MATLAB محاكات هذه الإشارات وفحص الطيف الترددي لها لبيان كيفية حدوث ظاهرة الارتداد (أو الالتباس) (aliasing) نتيجة لأخذ العينات بمعدلات أدنى من المعدل المطلوب. حيث تؤدي ظاهرة الارتداد إلى تشويه في الإشارات المنقولة مما يؤدي إلى تدهور أداء نظام التحكم وقد يسبب عدم استقراره. تسلط الدراسة الضوء على أهمية أخذ العينات بمعدلات مناسبة في أنظمة التحكم الرقمية لتجنب تأثيرات الارتداد وضمان تمثيل دقيق للإشارة، حتى يتخذ نظام التحكم القرارات المناسبة. توضح النتائج والرسوم البيانية المنتجة باستخدام MATLAB، العلاقة بين معدل القياس والارتداد ودقة الإشارة، مما يوفر أساساً للمختصين عند تصميم أنظمة التحكم الرقمية.

**الكلمات المفتاحية:** أخذ العينات، التحكم الرقمي، الارتداد، معدل نيكويست، طيف الإشارة، تحويلات فوريير، الإشارات المقطعة.

## 1. Introduction

Signal sampling is a fundamental process in digital signal processing (DSP) and digital control systems, involving the conversion of continuous-time signals into discrete-time sequences for analysis, estimation, and controller implementation. The Nyquist-Shannon Sampling Theorem states that a bandlimited analog signal can be perfectly reconstructed if the sampling frequency  $f_s$  is at least twice the highest frequency component  $f_m$  of the signal ( $f_s \geq 2f_m$ ) [1]. However, many real-world signals are not strictly bandlimited, and sampling below this critical rate causes aliasing overlapping frequency components that lead to distortion and potential instability in control loops [2].

Accurate sampling of sensor signals and control inputs is vital for digital control system stability and performance; insufficient rates can induce delays, degraded response, or instability [3, 4]. Oversampling, sampling well above the Nyquist rate, reduces aliasing and simplifies anti-aliasing filter design [5]. Contemporary digital control strategies also employ variable and adaptive sampling to balance computational load with control accuracy [6, 7, 8]. However, practical implementations must reconcile trade-offs among sampling frequency, computational complexity, and real-time constraints. This study addresses these challenges through a MATLAB-based comparative analysis of analog signal sampling at various rates relative to the Nyquist criterion. By examining the resulting frequency spectra, it exhibits the aliasing effects that arise from inadequate sampling and highlights the need for proper sampling strategies in digital control applications.

Figure 1 presents a block diagram illustrating the digital control signal flow, where the continuous-time plant output is sampled, processed digitally by a controller, and the digital control signal is converted back to an analog signal to actuate the plant.

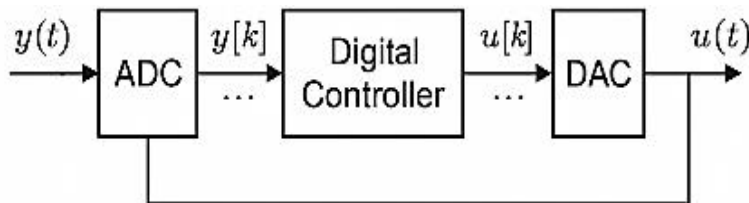


Fig. 1: Digital control system block diagram.

## 2. Proof of sampling theorem

Sampling theorem plays a crucial role in modern DSP. The theorem concerns about the minimum sampling rate required to convert a continuous time signal to a digital signal, without any or a loss of information. A continuous time signal can be represented in its samples and can be recovered back when sampling frequency  $f_s$  is greater than or equal to twice of the highest frequency component of message signal i. e.  $f_s \geq 2f_m$ . Consider a continuous time signal  $x(t)$ , the spectrum of  $x(t)$  is a band limited to  $f_m$  Hz, i.e. the spectrum of  $x(t)$  is zero for  $|\omega| > f_m$ . Sampling of input signal  $x(t)$  can be obtained by multiplying  $x(t)$  with an impulse train  $\delta(t)$  of period  $T_s$ . The output of multiplier is a discrete signal called sampled signal which is represented with  $y(t)$  as revealed in figure 2.

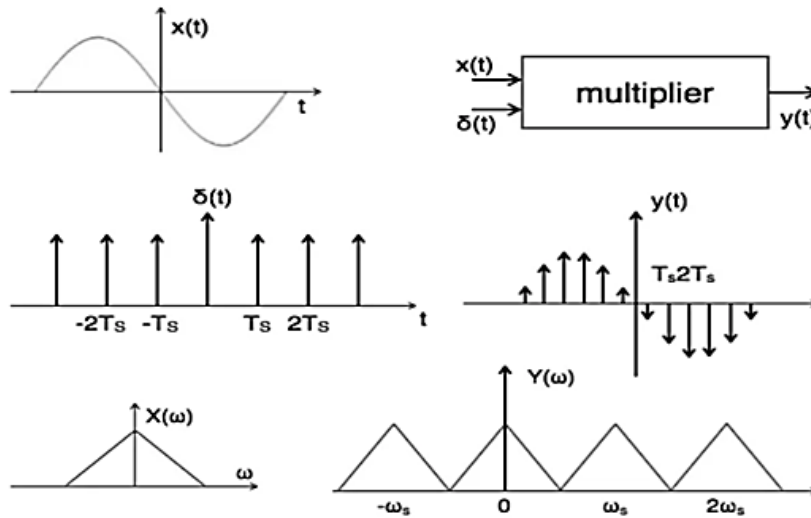


Fig. 2: Process of sampling signal.

Here, it can be observed that the sampled signal takes the period of the impulse function [2]. The process of sampling can be explained by the following mathematical equations:

$$\text{Sampled signal, } y(t) = x(t) \cdot \delta(t) \quad (1)$$

The trigonometric Fourier series representation of  $\delta(t)$  is given by:

$$\delta(t) = a_0 + \sum_{n=1}^{\infty} (a_n \cos n\omega_s t + b_n \sin n\omega_s t) \quad (2)$$

Where:

$$a_0 = \frac{1}{T_s} \int_{-\frac{T}{2}}^{\frac{T}{2}} \delta(t) dt = \frac{1}{T_s} \delta(0) = \frac{1}{T_s}, \delta(0)1 \quad (3)$$

$$a_n = \frac{2}{T_s} \int_{-\frac{T}{2}}^{\frac{T}{2}} \delta(t) \cos n\omega_s t dt = \frac{2}{T_s} \delta(0) \cos n\omega_s 0 = \frac{2}{T_s} \quad (4)$$

$$b_n = \frac{2}{T_s} \int_{-\frac{T}{2}}^{\frac{T}{2}} \delta(t) \sin n\omega_s t dt = \frac{2}{T_s} \delta(0) \sin n\omega_s 0 = 0 \quad (5)$$

Substituting above values in equation 2, yields:

$$\delta(t) = \frac{1}{T_s} + \sum_{n=1}^{\infty} \left( \frac{2}{T_s} \cos n\omega_s t + 0 \right) \quad (6)$$

Substituting  $\delta(t)$  in equation 1, we obtain:

$$y(t) = x(t) \left( \frac{1}{T_s} + \sum_{n=1}^{\infty} \left( \frac{2}{T_s} \cos n\omega_s t \right) \right) = \quad (7)$$

$$\frac{1}{T_s} (x(t) 2(\cos \omega_s t) x(t)) + 2(\cos 2\omega_s t) x(t) + 2(\cos 3\omega_s t) x(t) \dots$$

Taking the Fourier transform on both sides of equation 7, yields:

$$Y(\omega) = \frac{1}{T_s} (X(\omega) + (X(\omega - \omega_s) + (X(\omega + \omega_s) + (X(\omega - 2\omega_s) + (X(\omega + 2\omega_s) + \dots))$$

$$Y(\omega) = \frac{1}{T_s} \sum_{n=-\infty}^{\infty} X(\omega - n\omega_s) \quad (8)$$

Where  $n=0, \pm 1, \pm 2, \dots$

In order to reconstruct signal  $x(t)$ , input signal spectrum  $X(\omega)$  must be recovered from sampled signal spectrum  $Y(\omega)$ . This is possible only when there is no overlapping between the cycles of  $Y(\omega)$  [5]. Possibility of sampled frequency spectrum with different conditions are revealed in figure 3.

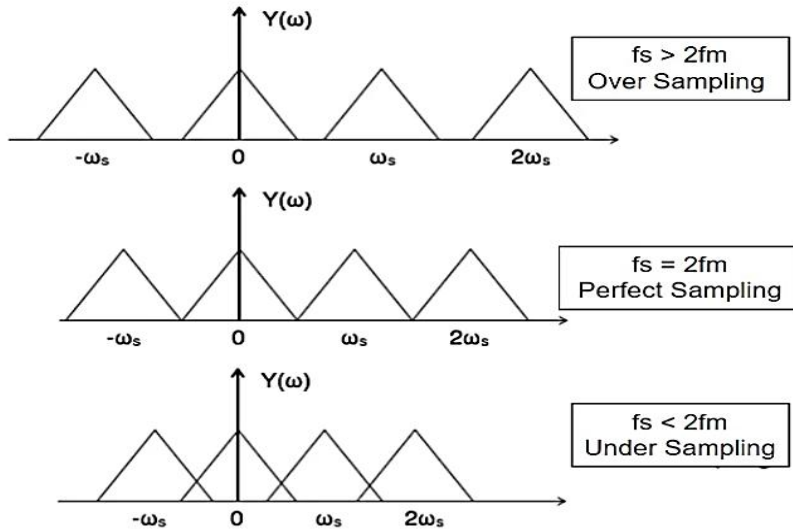


Fig. 3: Sampling process scenario.

### 3. How aliasing occurs

To obtain an insight into this phenomenon, Fourier transform of the sampled signal is analysed and compared with the Fourier transform of the analog (continuous) signal.

Let  $x_a(t)$  represents an analog signal with highest frequency component at  $\Omega_n$ , and set  $(t)$  represents a periodic impulse train, with a period  $T$  [9], that is:

$$s(t) = \sum_n \delta(t - nT) \quad (9)$$

$\delta(t)$  is the unit impulse function. If  $x_a(t)$  is sampled at a period  $T$ , the sampled signal,  $x_s(t)$ , can be represented as the product of the two [10], that is:

$$x_s(t) = x_a(t) \cdot s(t) = x_a(t) \cdot \sum_n \delta(t - nT) \quad (10)$$

Since multiplication in the time domain translates into convolution in the frequency domain, the relationship between the Fourier transforms of the three functions is given by:

$$X_s(j\Omega) = \frac{1}{2\pi} X_a(j\Omega) * S(j\Omega) \quad (11)$$

Where  $\Omega$  represents analog frequency. The Fourier transform of  $s(t)$ , the periodic impulse train, is a periodic impulse train in the frequency domain [3], that is:

$$S(j\Omega) = \frac{2\pi}{T} \sum_k \delta\left(\Omega - \frac{k \cdot 2\pi}{T}\right) = \frac{2\pi}{T} \sum_k \delta(\Omega - k\Omega_s) \quad (12)$$

Carrying out the convolution in the previous equation, results in:

$$X_s(j\Omega) = \frac{1}{T} \sum_k X_a(j\Omega - k\Omega_s) \quad (13)$$

Equation (13) implies that the Fourier transform of a uniformly sampled signal comprises infinitely many replicas of  $X_a(j\Omega)$ , each shifted by integer multiples of the sampling frequency  $\Omega_s$ . When  $f_s < 2f$  Nyquist, these replicas overlap, causing high-frequency content to fold into lower bands (aliasing) and rendering ideal reconstruction impossible. Conversely, if  $f_s \geq 2f$  Nyquist, no overlap occurs and a suitable low-pass filter can perfectly recover the original spectrum [2], [10]. Figure 4 depicts this effect on an analog signal's spectrum.

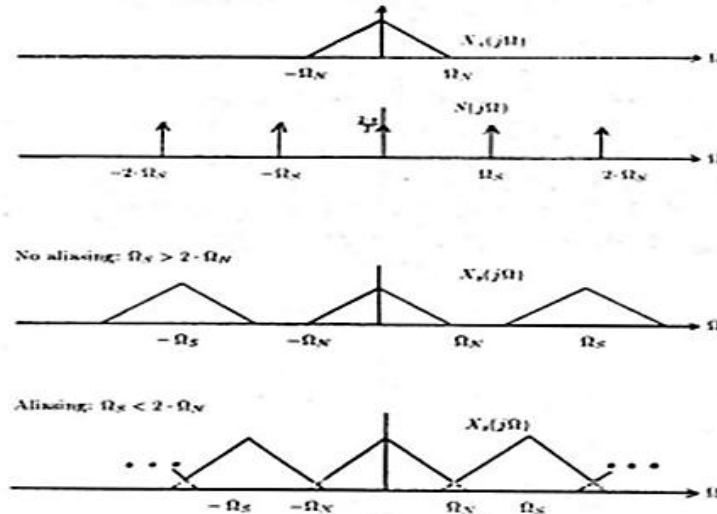


Fig. 4: Fourier Transform of an analog signal  $x_a(t)$ .

Aliasing can also be demonstrated in a simpler way, when we analyze the relationship between the sampled versions of a group of pure sinusoids [9]. Consider the continuous sinusoid of frequency  $\omega_0$  :

$$x(t) = \sin(\omega_0 t) \quad (14)$$

When sampled at a sampling period  $T$ , the resulted sampled sequence is:

$$x(n) = \sin(\omega_o nT), \quad n = 0, \pm 1, \pm 2, \dots \quad (15)$$

Now consider the group of sinusoids of frequency  $\omega$ , where:

$$\omega = \omega_o + \frac{2\pi k}{T}, \quad n = 0, \pm 1, \pm 2, \dots \quad (16)$$

When sampling any sinusoid signal at a sampling period  $T$ :

$$y(t) = \sin\left(\left(\omega_o + \frac{2\pi k}{T}\right)t\right) \quad (17)$$

This will result in a sequence which is identical to the sampled sequence of frequency  $\omega_o$ . To see that, we observe:

$$\begin{aligned} y(n) &= \sin\left(\left(\omega_o + \frac{2\pi k}{T}\right)nT\right) = \sin((\omega_o nT) + 2\pi kn) \\ &= \sin(\omega_o nT) \end{aligned} \quad (18)$$

A continuous signal  $x(t)$  and any sinusoid  $y(t)$  with frequency separated by an integer multiple of  $\Omega_s$  become indistinguishable when sampled at interval  $T$ . In practice, aliasing occurs as high frequency components fold into lower frequency bands, preventing accurate reconstruction [3], [4].

#### 4. Implementation and results

To investigate the effects of sampling rates and aliasing in signals, particularly within the context of digital control systems, set of simulations was conducted using MATLAB. The simulations aimed to illustrate how improper sampling distorts signals and how oversampling preserves fidelity. The procedure involved the following two parts:

##### A. Single-Frequency and Time Domain Analysis

###### 1. Signal definition:

A time vector  $t$  was created to span 2 seconds with a sampling interval  $T = 1/1000$  seconds, corresponding to a sampling frequency  $F_s = 1000$  Hz. Two cosine signals were generated using the  $\cos$  function:

- A 50 Hz cosine wave:  $x_1 = \cos(2 * \pi * 50 * t)$
- A 100 Hz cosine wave:  $x_2 = \cos(2 * \pi * 100 * t)$

Both signals were plotted using  $\text{plot}(t, x)$  to visualize their shapes and frequency contents.

## 2. Under-sampling Simulation

To demonstrate aliasing, the 50 Hz signal was regenerated using a lower sampling interval  $T = 1/200$  seconds ( $F_s = 200$  Hz). This under-sampled signal was plotted alongside the properly sampled version to highlight aliasing effects. Aliasing manifests as the sampled waveform appearing to contain incorrect frequency content.

## 3. Multi-Rate Comparison

To explore the effect of different sampling frequencies, a 50 Hz cosine signal was sampled at three rates: 100 Hz, 500 Hz, and 1000 Hz using the following MATLAB code:

- $F_{s1} = 100; F_{s2} = 500; F_{s3} = 1000;$
- $t1 = 0:1/F_{s1}:2; x_1 = \cos(2 * \pi i * 50 * t_1);$
- $t2 = 0:1/F_{s2}:2; x_2 = \cos(2 * \pi i * 50 * t_2);$
- $t3 = 0:1/F_{s3}:2; x_3 = \cos(2 * \pi i * 50 * t_3);$

These signals were visualized using MATLAB to illustrate the effects of under-sampling, critical sampling, and oversampling.

## 4. Visualization and Interpretation

This section offers a detailed interpretation of how sampling frequency affects signal fidelity in both time and frequency domains. Each figure corresponds to a specific discussion point, with implications for digital control system design where accurate sampling ensures stability and performance.

Figure 5 shows two cosine waves of 50 Hz and 100 Hz, both sampled at 1000 Hz (sampling time = 1 ms).

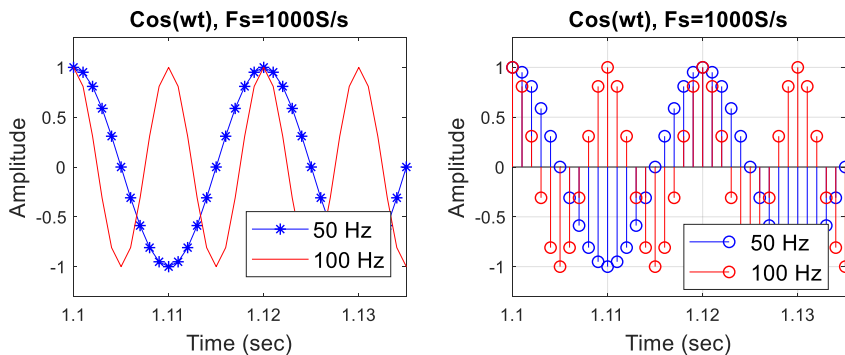


Fig. 5: Two cosine signals of 50Hz and 100Hz.

Figure 5 illustrates the distinction between two cosine waveforms of different frequencies sampled at 1000 Hz. The signal of 50 Hz has a period  $\tau = 20 \text{ ms}$ , while the 100 Hz signal has  $\tau = 10 \text{ ms}$ . the higher frequency signal completes more cycles over the same interval and is represented by fewer samples per cycle, reducing resolution. This illustrates the principle that while sampling above the Nyquist rate is essential, resolution and phase accuracy may still be affected at high frequencies [7].

To explore under-sampling, the 50Hz signal was also sampled at both 1000 Hz and 200 Hz and exhibited in Figure 6.

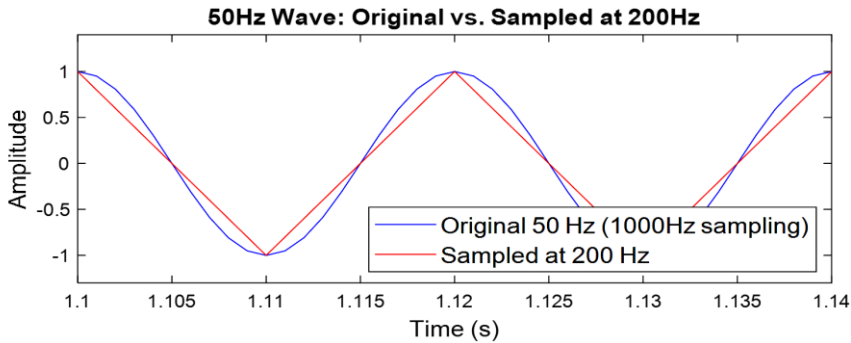


Fig.6: A cosine wave sampled at 200 Hz and 1000 Hz.

Figure 6 reveals that although the waveform sampled at 200 Hz retains the correct frequency, it appears less smooth and more polygonal, indicating fewer sampling points per cycle. This finding supports [8], which notes that sparse sampling distorts waveform appearance and may degrade system stability in digital control applications.

Further, the signal was sampled at 500 Hz and plotted in Figure 7, showing a compromise between resolution and efficiency.

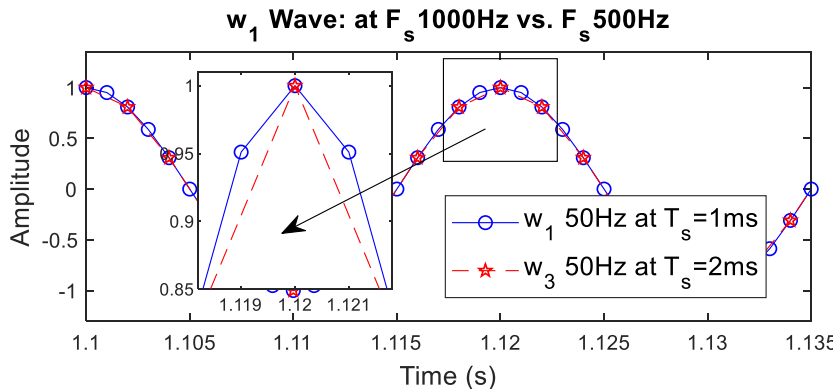


Fig.7: Cosine wave sampled at 500 Hz compared with at 1000 Hz

As depicted in Figure 7, at 500 Hz, the waveform is smoother than at 200 Hz, though not as precise as at 1000 Hz. This aligns with [11], highlighting that moderate oversampling can significantly reduce artifacts without the full cost of very high rates. To examine further oversampling, a new cosine signal of 50 Hz was sampled at 2000 Hz, and compared in Figure 8.

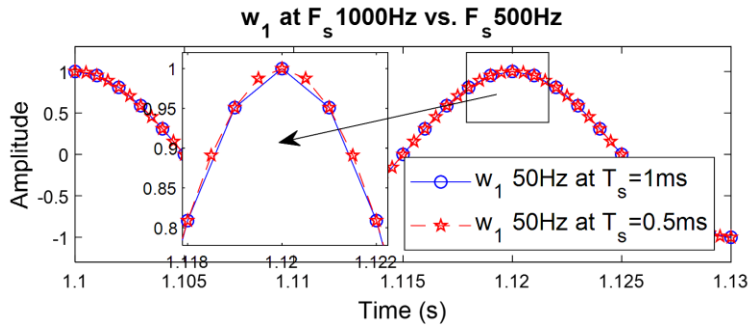


Fig. 8: Comparison of a 50 Hz signal sampled at 1000 Hz and 2000.

Figure 8 reveals that when the waveform sampled at 2000 Hz exhibits high smoothness and fidelity, but offers minimal structural improvement over the 1000 Hz version. While beneficial in applications like high-speed control or digital audio, such oversampling increases memory and computational demands [12]. These results reinforce modern literature findings [13–18], confirming that improper sampling (especially under-sampling) can destabilize control loops and degrade performance in feedback systems such as robotics and smart grids.

## B. Multi-Frequency and Frequency Domain Analysis

To extend the previous analysis, this section evaluates a composite signal consisting of multiple frequency components—more representative of real-world digital control and communication signals. This step is crucial in digital control applications and communication systems, where signals are typically modulated and contain a broad spectrum.

### 1. Composite Signal Generation

Four cosine signals of varying frequencies were simulated, that is  $f_1 = 50$  Hz,  $f_2 = 100$  Hz,  $f_3 = 500$  Hz and  $f_4 = 1000$  Hz. To emulate modulation, the 50 Hz signal was assigned a significantly larger amplitude ( $100 \times$  higher than the others) to act

as the carrier signal. A composite signal was then constructed by summing all four cosine signals:

$$w_1 = 100 * \cos(2 * \pi * 50 * t), \text{ (as the Carrier signal)}$$

$$w_2 = \cos(2 * \pi * 100 * t)$$

$$w_3 = \cos(2 * \pi * 500 * t)$$

$$w_4 = \cos(2 * \pi * 1000 * t)$$

$$w_t = w_1 + w_2 + w_3 + w_4$$

## 2. Sampling Parameters

Sampling frequency:  $F_s = 20000 \text{ Hz}$

Time vector:  $t = 0:1/F_s:5$

Number of samples:  $N = \text{length}(t)$

## 3. Frequency Spectrum Calculation

The FFT was computed as follows:

$X = \text{fft}(w_t)$ ;  $f = (0:N-1) * (F_s/N)$ ,  $f$  is the Frequency axis.

The FFT reveals each component's frequency content and amplitude, crucial for understanding signal behavior under various sampling conditions.

## 4. Resampling Scenarios

To test aliasing, the composite signal was resampled at:

$F_s/13 \approx 1538 \text{ Hz}$  (below Nyquist)

$F_s/11 \approx 1818 \text{ Hz}$  (near Nyquist)

$F_s/7 \approx 2857 \text{ Hz}$  (above Nyquist)

Each was plotted in time and frequency domains to observe distortion.

## 5. Flowchart and Simulation Summary

Figure 9 represents a flowchart summarizing MATLAB implementation steps-signal definition, time/frequency vector generation, FFT computation, and visualization.

The second part of the undertaking work simulates a composite waveform  $w_t$  Sampled initially at 20 kHz, its frequency spectrum, computed via FFT, demonstrates how high frequency content introduces rapid oscillations and informs realistic signal behavior. Based on earlier time domain analyses, this section focuses exclusively on  $w_t$  to illustrate the combined effects of multiple frequency components under a high sampling rate.

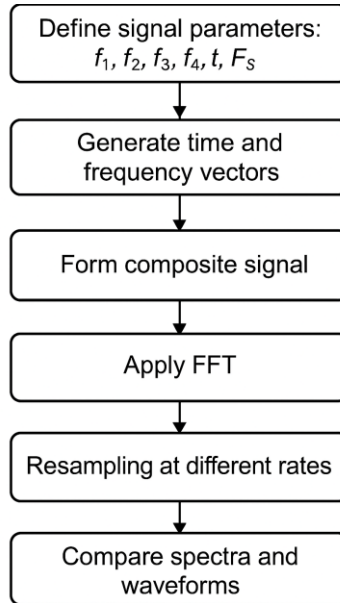


Fig.9: The scheme flowchart implemented in Matlab environment.

Figure 10 compares the base 50 Hz carrier and the full composite waveform  $w_t$ .

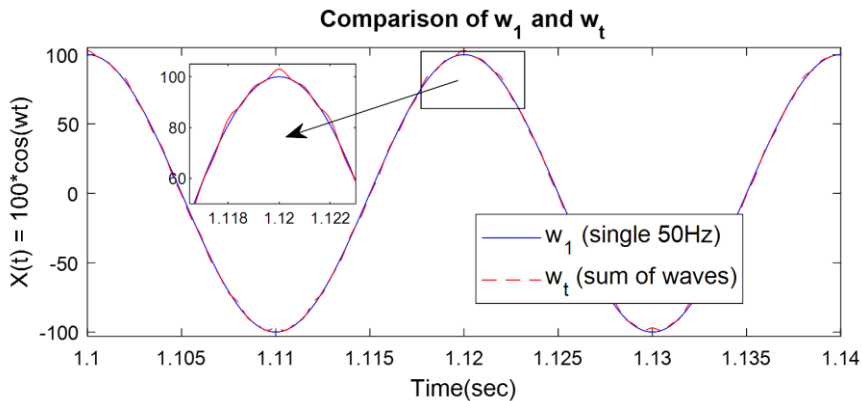


Fig.10: Time-domain view of  $w_1$  (50 Hz) and the composite signal  $w_t$ .

As illustrated in Figure 10, while the waveform appears smooth, its true frequency complexity is hidden. It exhibits a complex structure, indicating that the energy of the composite signal is distributed across its multiple frequency components, but does not significantly exceed the amplitude of the original carrier. The close amplitude values also suggest that the modulation process was well-balanced, avoiding over-modulation which could lead to distortion or signal

clipping. This characteristic is essential in amplitude-constrained transmission environments, such as analog communication and digitally modulated control signals [19]. To discover such complexity and to gain further insight, an FFT was applied. Figure 11 presents the frequency-domain view of  $w_1$  and  $w_t$ .

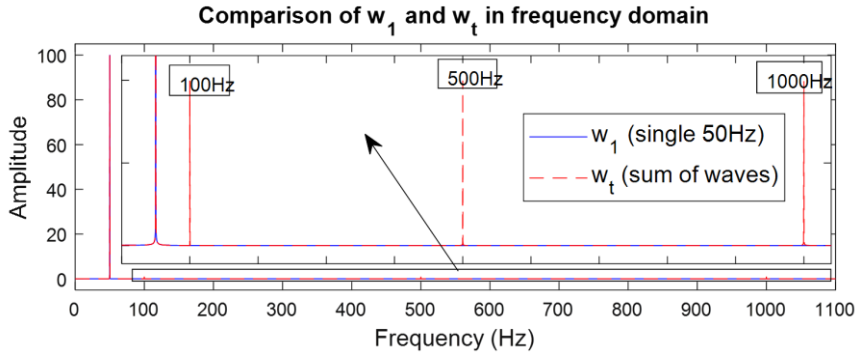


Fig. 11: Frequency-domain comparison of  $w_1$  and  $w_t$  using FFT.

Figure 11 reveals distinct spectral peaks at 50, 100, 500, and 1000 Hz, confirming the signal's modulation structure. This highlights how frequency-domain analysis complements time-domain insights by revealing hidden periodicities. The multiple frequency components reflect modulation techniques essential in digital control systems.

To evaluate the impact of sampling rate, the composite signal was resampled at  $F_s/7$ ,  $F_s/11$ , and  $F_s/13$ , then compared to the original. Figures 12 -14 show the effect of resampling in the time domain. Despite visual similarity, frequency content varies significantly.

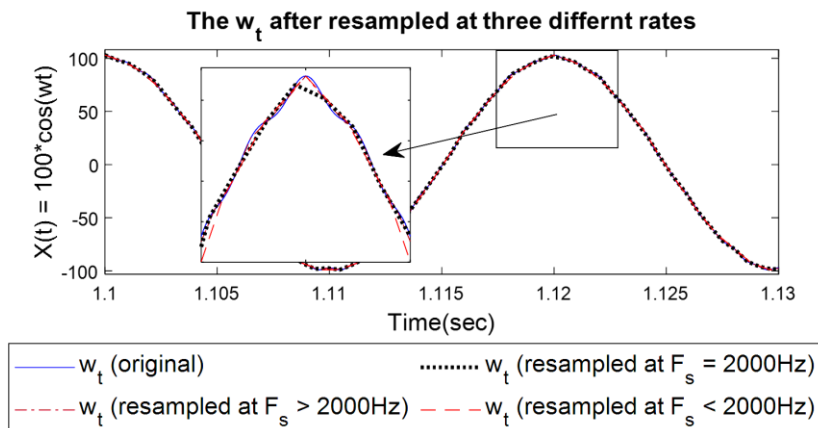


Fig.12: Time domain view of  $w_t$  at different resampling rates.

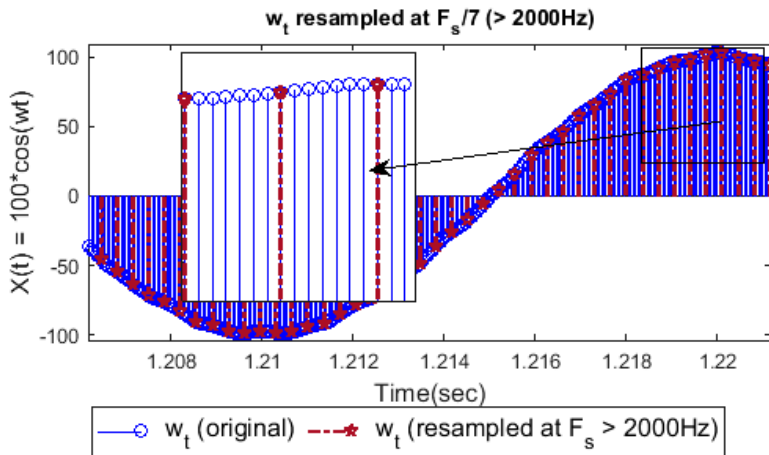


Fig.13: Zoomed view of  $w_t$  sampled at  $F_s/7$ .

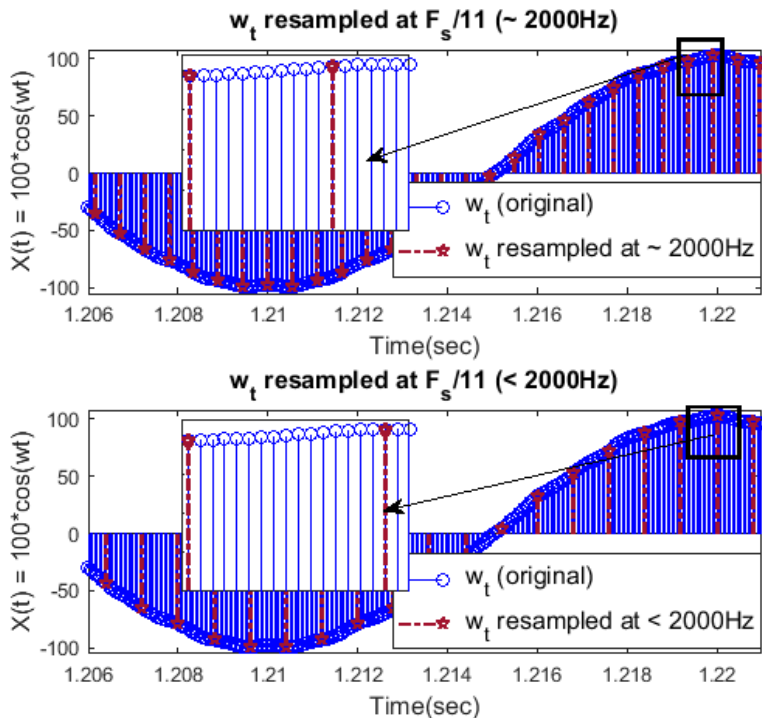


Fig.14:  $w_t$  sampled at  $F_s/11$  and  $F_s/13$ .

This again confirms a key point from earlier sections: time domain representation alone cannot adequately capture the effects of under-sampling. Figure 15 provides the FFT of each resampled signal, making the consequences explicit.

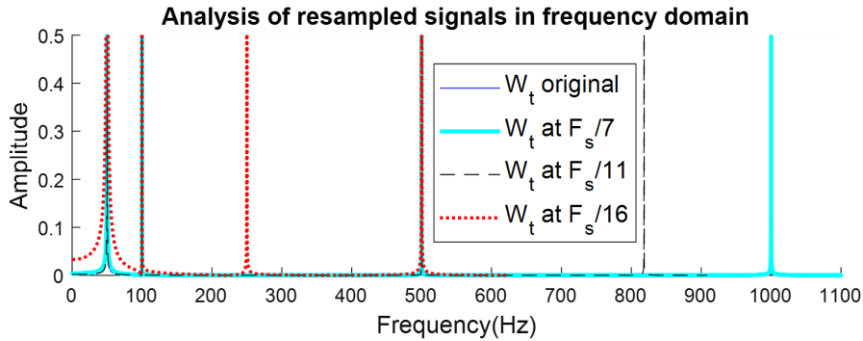


Fig.15: Frequency domain analysis of  $w_t$  after resampling.

Sampling at  $F_s/7$  preserves all frequency components, consistent with the Nyquist criterion. However, at  $F_s/11$ , aliasing becomes evident most notably with the 1000 Hz component, which is replaced by an erroneous 800 Hz signal. The distortion is more severe at  $F_s/13$ , where under-sampling results in significant frequency shifts and loss of original content.

This confirms that while time domain plots offer a superficial view, frequency domain analysis is essential for detecting aliasing and ensuring signal integrity, especially in digital control applications. Furthermore, it reinforces our earlier finding that correct sampling is not merely a mathematical requirement but a practical necessity for preserving informational accuracy in digitally processed systems.

This behavior substantiates the Nyquist-Shannon sampling theorem, which states that the sampling frequency must be at least twice the highest frequency component present in the signal to avoid aliasing [20]. As observed, insufficient sampling leads to misrepresentation of signal content, potentially corrupting any control or communication data encoded in those frequencies. Conversely, oversampling—while resource-intensive ensures accurate reconstruction and robustness against quantization noise.

These findings bear practical implications for digital control systems and signal transmission networks. Signal fidelity must be balanced against computational and storage constraints, especially in embedded and real-time systems. Consequently, choosing an optimal sampling rate is a design trade-off, where engineers must consider system bandwidth, power limitations, and processing capacity [21].

## 5. Conclusion

This study explored the influence of sampling rates on controlled signal fidelity through both time-domain and frequency-domain analysis. It was demonstrated that:

- Time-domain views offer limited insight, especially in complex signals.
- FFT-based frequency analysis is essential for detecting aliasing and spectral distortion.
- Under-sampling leads to significant information loss and control degradation.
- Oversampling improves accuracy but increases computational load.

In practical systems, a trade-off must be struck between sampling fidelity and resource efficiency. The findings underscore the importance of adaptive and intelligent sampling strategies for modern control systems, particularly in embedded or resource-constrained environments.

Future research could include:

- Intelligent sampling via machine learning.
- Wavelet and non-stationary signal analysis.
- Hardware-in-the-loop validation.

By bridging theory with simulation, this work contributes to the advancement of robust and efficient digital control and signal analysis systems.

## 6. References

- [1] E. C. Ifeachor, B. W. Jervis, Digital Signal Processing: A Practical Approach, 2nd ed., Pearson Education, 2002.
- [2] A. V. Oppenheim, R. W. Schaffer, Discrete-Time Signal Processing, 3rd ed., Pearson, 2010.
- [3] K. J. Åström and B. Witten mark, Computer-Controlled Systems: Theory and Design, 3rd ed., Prentice Hall, 1997.
- [4] G. C. Goodwin, S. F. Graebe, M. E. Salgado, Control System Design, Prentice Hall, 2001.
- [5] S. Haykin, B. Van Veen, Signals and Systems, 2nd ed., Wiley, 2003.
- [6] P. P. Vaidyanathan, "Multirate digital signal processing for control applications," IEEE Control Systems Magazine, vol. 31, no. 2, pp. 32-45, 2011.

- [7] Tian, Y., Wu, M., & Sun, J. (2021). "Adaptive Sampling in Non-Stationary Signal Environments." *IEEE Transactions on Signal Processing*, 69, 1342–1355.
- [8] Zhang, R., & Liu, Y. (2022). "Sampling Rate Impact on Time-Frequency Representations in Digital Control." *Journal of Control Engineering and Technology*, 10(3), 215–224.
- [9] M. Al-Saleh, N. Sulaiman, "Fractional Fourier Transform and Its Applications in Signal Processing: A Review," *Signal Processing*, vol. 167, 2020, 107286.
- [10] J. Wang, Y. Ma, "Oversampling and Interpolation Techniques for Improved Signal Reconstruction," *IEEE Transactions on Circuits and Systems I*, vol. 67, no. 9, pp. 3057-3066, 2020.
- [11] Abdelkarim, A., Yang, C., & Hashimoto, S. (2023). "Digital Signal Integrity in Embedded Systems with Limited Sampling Rates." *IEEE Access*, 11, 28790–28805.
- [12] Tan, K. C., Lim, C. S., & Chan, M. (2023). "Efficient Oversampling Methods in Real-Time Signal Processing." *Signal Processing Letters*, 30, 450–455.
- [13] Isermann, R. (2010). *Digital Control Systems*. Springer Science & Business Media.
- [14] Chen, T., & Francis, B. A. (1995). *Optimal Sampled-Data Control Systems*. Springer.
- [15] Yu, W., & Kaynak, O. (2022). "Sampling rate effects on digital twin-driven control systems," *IEEE Transactions on Industrial Informatics*, 18(3), 1511–1520.
- [16] Ramezanifar, A., & Jin, X. (2023). "Adaptive digital control under resource constraints," *IEEE Control Systems Magazine*, 43(1), 54–66.
- [17] Li, P., et al. (2022). "Digital control of power converters with optimal sampling design," *IEEE Journal of Emerging and Selected Topics in Power Electronics*, 10(4), 4224–4236.
- [18] Zhang, Y., & Ren, W. (2021). "Sampling strategies for real-time feedback in robotic systems," *IEEE Transactions on Robotics*, 37(5), 1412–1425.
- [19] Proakis, J.G. & Manolakis, D.G. (2021). *Digital Signal Processing: Principles, Algorithms, and Applications*. Pearson Education.

- [20] Oppenheim, A.V., & Schafer, R.W. (2014). Discrete-Time Signal Processing. Pearson.
- [21] Lyons, R.G. (2011). Understanding Digital Signal Processing, 3<sup>rd</sup> Edition. Prentice Hall.